CANCER

Copyright © 2022 The Authors, some rights reserved; exclusive licensee American Association for the Advancement of Science. No claim to original U.S. Government Works

Simultaneous analysis of mutations and methylations in circulating cell-free DNA for hepatocellular carcinoma detection

Pei Wang[1]†, Qianqian Song[1]†, Jie Ren[2]†, Weilong Zhang[1,3]†, Yuting Wang[1,4], Lin Zhou[2], Dongmei Wang[1,4], Kun Chen[4], Liping Jiang[1], Bochao Zhang[2], Wanqing Chen[5], Chunfeng Qu[1,4]*, Hong Zhao[6]*, Yuchen Jiao[1]*

Cell-free DNA (cfDNA)–based liquid biopsy is a promising approach for the early detection of cancer. A major hurdle is the limited yield of cfDNA from one blood draw, limiting the use of most samples to one test of either mutation or methylation. Here, we develop a technology, Mutation Capsule Plus (MCP), which enables multiplex profiling of one cfDNA sample, including simultaneous detection of genetic and epigenetic alterations and genome-wide discovery of methylation markers. With this technology, we performed de novo screening of methylation markers on cfDNA samples from 30 hepatocellular carcinoma (HCC) cases and 30 non-HCC controls. The methylation markers enriched in HCC cfDNA were further profiled in parallel with a panel of mutations on a training cohort of 60 HCC and 60 non-HCC cases, resulting in an HCC detection model. We validated the model in an independent retrospective cohort with 58 HCC and 198 non-HCC cases and got 90% sensitivity with 94% specificity. Furthermore, we applied the model to a prospective cohort of 311 asymptomatic hepatitis B virus carriers with normal liver ultrasonography and serum AFP concentration. The model detected four of the five HCC cases in the cohort, showing 80% sensitivity and 94% specificity. These findings demonstrate that the MCP technology has potential for the discovery and validation of multiomics biomarkers for the noninvasive detection of cancer. This study also provides a comprehensive database of genetic and epigenetic alterations in the cfDNA of a large cohort of HCC cases and high-risk non-HCC individuals.

INTRODUCTION

Hepatocellular carcinoma (HCC) is the fifth most common and the third most lethal cancer worldwide (*1*). The 5-year survival rate for advanced-stage HCC is only 12% because the therapies available have limited efficacy (*2*). The most efficient way to cure this disease is to detect it in the early stage so that the tumor can be promptly removed surgically (*3*, *4*). Thus, an efficient screening method that detects HCC in a surgically resectable stage with high accuracy is needed.

Among the alternative screening methods considered, liquid biopsy based on cell-free DNA (cfDNA) has emerged as a promising approach for noninvasive diagnosis in clinical applications (*5*, *6*). Previous studies have identified potential cancer diagnostic markers, such as somatic mutations (*7*), methylation markers (*8*, *9*), the cfDNA size distribution (*10*, *11*), and cfDNA breakpoints (*12*, *13*).

In HCC, multiple studies have confirmed the feasibility of mutation detection using liquid biopsy (*14*–*19*). However, the detection of low-frequency mutations in low-yield cfDNA could be difficult because of sampling issues. For example, a mutation with a 0.01% frequency cannot be confidently detected when only 3000 copies (equal to 10 ng) of cfDNA are profiled. Such false-negative detection results could be especially common in patients with early-stage cancer (*20*). DNA methylation changes are among the earliest molecular alterations to occur during cancer progression, and aberrant DNA methylation changes, including the hypermethylation of CpG islands (CGIs), are hallmarks of nearly all human cancer types, including HCC (*21*–*23*). Detection of cfDNA methylation has emerged as a promising noninvasive approach for the diagnosis, prognosis, and monitoring of cancers (*24*). Bisulfite sequencing is considered the gold standard for DNA methylation analysis; however, the harsh conditions of this method could cause substantial DNA damage, decreasing the detectability of the cfDNA and the sensitivity of the assay (*25*, *26*).

According to previous studies, combinational profiling of multiomics biomarkers, such as methylation, mutation, and protein markers, may increase the performance of cancer detection (*7*, *10*, *14*, *27*). However, most cfDNA profiling technologies can detect only one type of biomarker, whereas the cfDNA yield from one blood draw is not sufficient to support multiple tests. Thus, most previous studies have focused on only one type of biomarker at a time, and it is difficult to compare the performance of biomarkers profiled in different cohorts from different studies or to combine biomarkers to develop a better algorithm for detecting cancer.

[1]State Key Laboratory of Molecular Oncology, National Cancer Center/National Clinical Research Center for Cancer/Cancer Hospital, Chinese Academy of Medical Sciences and Peking Union Medical College, Beijing 100021, China. [2]Fanshengzi Clinical Laboratory, Beijing 102206, China. [3]Department of Hematology, Lymphoma Research Center, Peking University Third Hospital, Beijing 100191, China. [4]Immunology Department, National Cancer Center/National Clinical Research Center for Cancer/Cancer Hospital, Chinese Academy of Medical Sciences and Peking Union Medical Colleges, Beijing 100021, China. [5]Office of Cancer Screening, National Cancer Center/ National Clinical Research Center for Cancer/Cancer Hospital, Chinese Academy of Medical Sciences and Peking Union Medical College, No.17 Pan-jia-yuan South Lane, Chaoyang District, Beijing 100021, China. [6]Department of Hepatobiliary Surgery, National Cancer Center/Cancer Hospital, Chinese Academy of Medical Sciences and Peking Union Medical College, Beijing 100021, China.
*Corresponding author. Email: jiaoyuchen@163.com (Y.J.); zhaohong9@sina.com (H.Z.); quchf@cicams.ac.cn (C.Q.)
†These authors contributed equally to this work.

Downloaded from https://www.science.org on November 25, 2022

To address this problem, we developed the Mutation Capsule Plus (MCP) technology, supporting parallel profiling of mutations and methylation changes (MCP profiling) and de novo discovery of methylation markers through CpG tandems target amplification (CTTA). The MCP technology also enabled multiplex tests on a single cfDNA sample without sacrificing sensitivity, which can occur when splitting a cfDNA sample for multiple reactions. We applied the MCP technology to the discovery, training, and validation of a liquid biopsy assay for the detection of HCC. This comprehensive profiling approach allowed a comparison of cfDNA-based biomarkers, revealing the complementary pattern of the methylation and mutation biomarkers for HCC detection.

RESULTS

Design of the MCP technology

To comprehensively analyze cfDNA, we aimed to develop a new technique that supports the following features: (i) parallel profiling of genetic and epigenetic alterations in the same reaction; (ii) recurrent profiling of a single cfDNA sample without sacrificing sensitivity; and (iii) genome-wide discovery of methylation markers. To achieve these aims, this method took the approach of methylation-sensitive restriction enzyme treatment on the original cfDNA template rather than bisulfite conversion so that both mutational and methylation information could be preserved. To do this, cfDNA was digested with the methylation-sensitive restriction enzyme Hha I, which cleaves only unmethylated cfDNA at the 4–base pair (bp) GCGC restriction site. After digestion, the cfDNA sample was ligated with a customized adapter (figs. S1A and S2) with DNA barcodes and amplified for a whole-genome library (pre-MCP library) (fig. S1A). In the pre-MCP library, the methylation status of a GCGC site was transferred to the digestion status, where methylated cfDNA kept intact, and unmethylated cfDNA was digested into shorter fragments ending with the GCGC site. During the construction of the pre-MCP library, each original cfDNA molecule was assigned a unique identifier (UID) and amplified to more than 100 copies. Ten percent of the pre-MCP library was sufficient to represent the original cfDNA molecules, and the pre-MCP library from a cfDNA sample could support 10 profiling reactions.

To profile mutation and methylation changes in parallel, gene-specific (GS) primers were designed to target the coding regions or regions adjacent to Hha I digestion sites. A universal primer matching the adapter sequence was used to amplify the target regions with the GS primers from the pre-MCP library (fig. S1B). For the primers targeting the Hha I cutting sites, the amplified fragments from unmethylated cfDNA were short in size and ended with the digestion site, whereas those from methylated cfDNA were full-length cfDNA covering the digestion site. Thus, the coding regions and Hha I regions could be amplified in the same reaction to profile mutation and methylation changes in parallel (fig. S1B). A total of 281,154 GCGC restriction sites were identified in the 26,641 CGI regions in the human genome according to the University of California, Santa Cruz genome database at the time of this study. In total, 94% (25,149 of 26,641) of the CGIs contained at least one Hha I restriction site and thus were accessible by our method. On the other hand, clustered restriction sites were rare in the coding regions, and the detection of mutations was only slightly affected by Hha I digestion. One pre-MCP library could support multiple MCP profiling reactions with different panels of mutation and methylation markers. In particular, we could profile one pre-MCP library with two sets of primers in two reactions, each amplifying the target regions from one direction. Targeting from both sides made more original cfDNA molecules detectable, thus increasing the sensitivity to detect low-frequency mutations in low-yield cfDNA samples (figs. S1B and S3).

We also aimed to apply the pre-MCP library for the de novo discovery of methylation markers through CTTA (fig. S1B). To do this, we designed a set of primers with a GCGC sequence at the 3′ end and used the primers to amplify the pre-MCP library with the universal primer. The methylated cfDNA with an intact 4-bp GCGC restriction site would be amplified with the downstream cfDNA sequence, whereas the digested unmethylated cfDNA would not be amplified. The methylated DNA would thus be enriched in the amplified library and detected by deep sequencing. We screened the CpG tandems highly enriched in CGIs in the human genome and designed a five-primer set by joining multiple CpG tandems targeting (CTT) primers (table S1) ending with the Hha I digestion site for the amplification of the pre-MCP library. Seventy-nine percent (21,032 of 26,641) of CGIs in the human genome could be covered by this approach.

Performance of MCP in mutation detection

The performance of MCP was first evaluated for the detection of mutations. A panel targeting 10 mutation sites (panel A, table S1) for MCP profiling was designed. We performed MCP to target panel A on negative control DNA isolated from the white blood cells (WBC) of a healthy donor. We found that the error frequency decreased when the sequencing data were filtered with the algorithm based on the DNA barcode and UID family (fig. S4A). Last, two or more UID families were required to call a mutation (*13*, *28*, *29*).

Next, we analyzed the sensitivity of MCP in the detection of mutations. To do this, we performed MCP on standard reference samples by spiking HD753 reference DNA with known mutations in WBC DNA from healthy controls. A total of 104 standard reference samples were analyzed with panel A, with four to eight replicates of each combination of an allele fraction (AF) (0.1, 0.050, 0.025, and 0%) and DNA input (5, 10, 20, 40, and 100 ng). In the reference samples, we achieved a mutation-level sensitivity of 100% at 0.1% AF, 100% at 0.05% AF, and 97.5% at 0.025% AF when starting with 100 ng of input DNA. When starting with 40 ng of input DNA, the sensitivities were 100% at 0.1% AF, 95% at 0.05% AF, and 73.8% at 0.025% AF (Fig. 1A and data file S1). None of the candidate mutations were detected in the wild-type samples (100% specificity at 0% AF). In addition, MCP technology showed strong performance for low-frequency mutations in low-yield cfDNA samples by achieving 93.8% sensitivity at 0.1% AF with 10 ng of input DNA or 67.5% sensitivity with 5 ng of input DNA. When starting with 20 ng of input DNA, we could accurately detect mutations at an AF of 0.025% with a sensitivity of 68.8% (Fig. 1A and data file S1). The performance (72.5% sensitivity for 0.1% AF point mutations with 5-ng DNA) was better than those reported in previous studies, which showed sensitivity of 50.8% at 0.125% AF point mutations with 7 to 8 ng of input DNA (*30*).

One potential reason for the improved sensitivity was that MCP supports the targeting of a mutation from both directions in two reactions so that almost all cfDNA molecules could be amplified and sequenced. To validate the benefit of this feature, the sensitivity

Downloaded from https://www.science.org on November 25, 2022

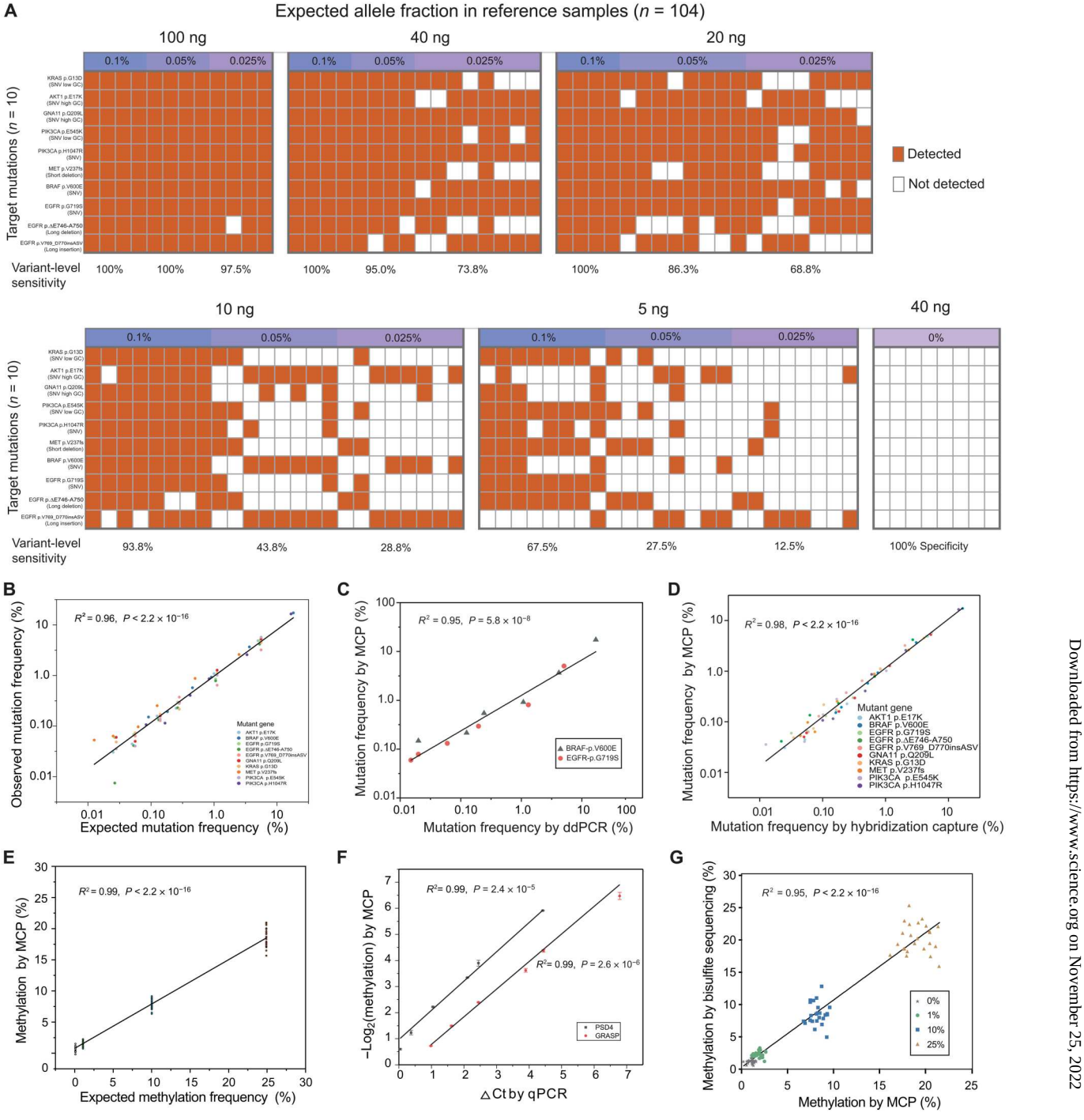

Fig. 1. Analysis of MCP performance in the detection of mutation and methylation. (**A**) Sensitivity and specificity in detecting mutations across 104 reference samples and 10 mutations. Each row corresponds to a targeted mutation, and each column corresponds to a single sample analyzed at the identified allele fraction (AF). SNV, single-nucleotide variant. (**B**) Comparison of variant AFs observed using MCP (*y* axis) with expected variant AFs (*x* axis). For each variant, the mean observed AF across all replicates ($n = 3$) at the same expected AF is presented. The HD753 reference DNA sample was diluted with white blood cell (WBC) DNA to obtain a gradient of seven concentrations (mutation AF = 0, 0.020, 0.050, 0.125, 0.250, 1.00, and 5.00%), and each dilution gradient was profiled with MCP. (**C**) Consistency of MCP (*y* axis) with digital droplet PCR (*x* axis) in the detection of mutations. Triangles and circles represent two hotspot mutations profiled. $n = 3$ biological replicates. (**D**) Correlation of the mutation frequencies measured by MCP (*y* axis) and hybridization-based capture sequencing (*x* axis). Different colors indicate different target mutation sites. $R^2 = 0.98$. $n = 3$ biological replicates. (**E**) Consistency of the expected frequency and the observed amount detected by MCP in the methylation detection assay; $R^2 = 0.99$. $n = 3$ biological replicates. (**F**) Correlation between the methylation amount and ΔCt values (qPCR) of two methylated sites. The methylation was obtained from MCP, and the ΔCt value was obtained from the qPCR assay. $n = 3$ biological replicates. (**G**) Correlation between MCP and bisulfite-based sequencing methods in the detection of methylation at different methylation frequencies. Twenty-four methylation sites were analyzed at each methylation frequency. Each dot represents the mean methylation frequency across all replicates ($n = 3$).

Downloaded from https://www.science.org on November 25, 2022

of a single reaction sequencing the 10 mutation sites from a single direction in the reference samples was analyzed. The results indicated that the MCP strategy of sequencing mutations from both sides showed higher sensitivity than the approach sequencing mutations from a single side, especially for low-frequency mutations (fig. S4B and data file S1). The comparison further confirmed the strength of MCP in the detection of genetic variants.

In addition to single-nucleotide variant mutations, MCP was also able to detect complex mutations, such as long indels (Fig. 1A and data file S1). MCP did not detect any additional mutations other than the known mutations in the targeted region in these samples, confirming the noise-filtering effect of the UID-based algorithm.

Furthermore, a more comprehensive gradient dilution of the reference sample HD753 DNA was analyzed to determine the performance of MCP in detecting mutations (AF = 0, 0.025, 0.050, 0.125, 0.250, 1.00, and 5.00%). The data showed a strong linear correlation between the expected AFs and the observed AFs by MCP profiling [coefficient of determination (R^2) = 0.96, $P < 2.2 \times 10^{-16}$; Fig. 1B and data file S2]. The results of digital droplet polymerase chain reaction (PCR) at two hotspot mutations (EGFR-p.G719S and BRAF-p.V600E) were compared with MCP profiling on reference samples at different AFs (AF = 0, 0.025, 0.050, 0.125, 0.250, 1.00, and 5.00%). The correlations between the two methods were high for all the tested conditions ($R^2 = 0.95$, $P = 5.8 \times 10^{-8}$; Fig. 1C).

Many liquid biopsy studies using cfDNA to detect cancer are based on the hybridization-based methods to enrich targets of interest. Because MCP is an amplification-based enrichment method, a head-to-head comparison of these two methods was conducted on the same pre-MCP library from the standard reference samples. The two methods showed strong consistency in all tests, including those on low-frequency mutations ($R^2 = 0.98$, $P < 2.2 \times 10^{-16}$; Fig. 1D and data file S2). Therefore, the MCP technology could detect genetic variants without introducing detectable false-positive mutations.

Performance of MCP in methylation detection

To validate the performance of MCP in detecting methylation changes, 24 standard reference samples were produced by spiking fully methylated human genomic (FMG) DNA into nonmethylated human genomic (NMG) DNA in a series concentration (25, 10, 1, and 0%). A multiplexed panel (panel B, table S1) targeting 24 methylation sites was designed, and MCP was applied to analyze the methylation. The results showed a linear correlation between the expected methylation frequency and that obtained from MCP ($R^2 = 0.99$, $P < 2.2 \times 10^{-16}$; Fig. 1E and data file S3). At all 24 methylation sites, the 1% FMG dilution sample showed a significantly higher methylation than the 0% methylation sample (NMG DNA) ($P < 0.0001$, Wilcoxon signed-rank test) (fig. S4C), indicating that all methylation sites could be detected at a frequency of 1%. MCP was reproducible in the detection of methylation changes because the methylation detection yielded significant consistency between two replicates at all methylation sites tested ($R^2 = 0.99$, $P < 2.2 \times 10^{-16}$; fig. S4D). Furthermore, the performance of MCP and real-time quantitative PCR (qPCR) to detect methylation at a single methylation site was compared. Assays targeting two methylation sites were designed on the basis of bisulfite treatment and qPCR. The threshold cycle (Ct) values obtained using qPCR were applied to measure the fraction of methylation. The Ct values were significantly consistent with the methylation calculated using the MCP technology for each sample ($R^2 = 0.99$, $P = 2.4 \times 10^{-5}$ and $R^2 = 0.99$, $P = 2.6 \times 10^{-6}$, respectively) (Fig. 1F), which further confirmed the reliability of MCP in detecting methylation changes.

The performance of MCP was further evaluated in a larger panel of multiple methylation regions compared with the methylation detection method based on bisulfite sequencing. The same target regions were analyzed with the bisulfite-based assay. MCP technology showed consistency with the bisulfite-based method, and the methylation calculated from MCP showed a linear correlation with the bisulfite-based method ($R^2 = 0.95$, $P < 2.2 \times 10^{-16}$; Fig. 1G and data file S3).

Performance of mutation and methylation profiling in multiplex tests

We next tested the ability of an aliquot of a pre-MCP library to represent the original cfDNA to ensure that the MCP technology could support multiple rounds of profiling. To do this, we compared the results of three replicates of mutation/methylation profiling on a single pre-MCP library prepared from one cfDNA sample of a patient with HCC, where 10% of the pre-MCP library was used in each replicate. A panel targeting genes encoding tumor protein p53 (*TP53*) and telomerase reverse transcriptase (*TERT*) mutations and 21 methylation sites (panel C, table S1) was profiled by MCP (*31*, *32*). The alteration frequencies were highly consistent among all three replicates (Fig. 2A). In addition, UIDs were used to track the original cfDNA molecule. The UID families identified in the three replicates of MCP were largely overlapping, with 76% of the UID families being shared by all three replicates (Fig. 2B). In this case, one aliquot (10%) of the MCP library could represent most of the original cfDNA molecules (Fig. 2B). Furthermore, the same amount of the original cfDNA was used for an MCP assay without whole-genome amplification, in which the cfDNA-adapter ligation product was directly amplified with GS primers (*12*). The yield of UID families identified in the MCP profiling directly on the ligation product was not significantly different to that from one reaction on an aliquot (10%) of the pre-MCP library (Fig. 2, C and D). Thus, an aliquot of the pre-MCP library was sufficient to profile the genetic alterations with sensitivity comparable to the direct analysis of the original cfDNA sample. The remainder of the pre-MCP libraries could be used in additional MCP profiling reactions with different panels of biomarkers or to further improve the sensitivity with an additional reaction using primers targeting from the other side.

Development of the HCC detection model

We developed an HCC detection model with two classes of biomarkers: (i) epigenetic alterations at the methylation sites that were frequently hypermethylated in the cfDNA of patients with HCC and (ii) genetic alterations prevalent in HCC tumors, including mutations in *TP53*, *CTNNB1*, and *TERT*, as well as hepatitis B virus (HBV) integration, which is considered as a potential biomarker for the detection of HCC (*10*, *14*, *33*, *34*). In total, 148 patients with HBV-associated HCC and 288 HBV carriers without HCC (non-HCC control) were enrolled. The study workflow was shown in fig. S5.

For the de novo discovery of methylation markers of HCC, we first performed CTTA (panel D, table S1) on the pre-MCP libraries generated from the cfDNA of 30 patients with HCC and 30 non-HCC individuals. By comparing the HCC and non-HCC groups,

Downloaded from https://www.science.org on November 25, 2022

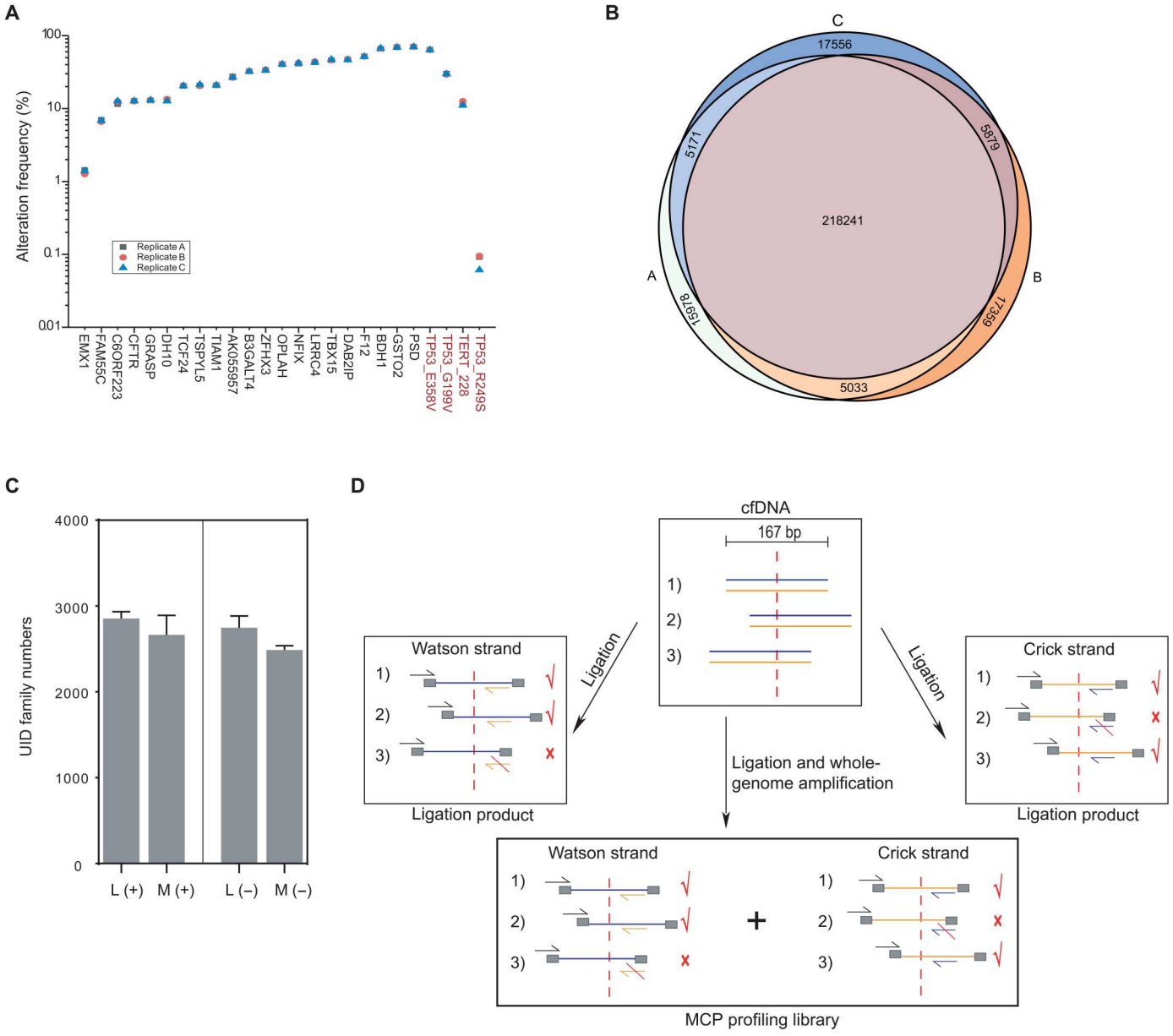

Fig. 2. The performance of multiple tests in one pre-MCP library. (**A**) Alteration frequency of three MCP replicates from the same pre-MCP library. The dot plot shows the frequency of a mutation or methylation marker. The *x* axis indicates mutation (red) and methylation markers. (**B**) Venn plot of UID family numbers detected in three replicates of targeted sequencing prepared from the same pre-MCP library. (**C**) Comparison of UID family numbers in two forms of MCP profiling libraries derived from the pre-MCP library or adapter ligation product. "L" indicates the MCP profiling library amplified directly from the adapter ligation product. "M" indicates the MCP profiling library amplified from an aliquot of the whole-genome pre-MCP library. "+" and "−" indicate specific primers designed as upstream or downstream to the target region. $n = 3$ biological replicates. (**D**) Comparison of amplification-based enrichment from two directions with that from one direction. A percentage of cfDNA molecules in the ligation product could not be amplified by primers from only one direction. On the other hand, all cfDNA molecules in a pre-MCP library could be amplified efficiently through two reactions with two sets of primers in both directions. The blue and yellow lines indicate the Watson and Crick strands of cfDNA, respectively. The gray square indicates the adapter sequence. The black primer is a universal primer targeting the adapter sequence, and the yellow and blue primers target the Watson and Crick strands, respectively.

we identified 1224 CGIs and 1309 GCGCs that were significantly hypermethylated in the cfDNA of the HCC group (fold change >4, $P < 0.001$, one-tailed Mann-Whitney test). Considering the degree of difference between the HCC and non-HCC groups and the design of the MCP targeting primers, we selected 56 markers for further analyses (fig. S6 and data file S4). In addition, we selected 22 methylation biomarkers reported to have diagnostic value for HCC in previous studies (*8*, *31*, *32*, *35*, *36*). Fourteen of the 22 methylation biomarkers were overlapped with the 56 markers found by CTTA. Together, we designed a panel targeting 64 methylation markers for MCP profiling (fig. S7). The panel also included the coding regions of *TP53*, *CTNNB1*, the promoter region of *TERT*,

Downloaded from https://www.science.org on November 25, 2022

and the full-length of HBV genome that was used to detect HBV integration. A total of 120 samples were assigned to the training cohort (60 HCC and 60 non-HCC) to profile the markers for the liquid biopsy detection of HCC. The built-in feature importance of the random forest algorithm was applied to identify the top-performing methylation markers in the training cohort. We chose the top 10 markers that showed differential hypermethylation in HCC cases versus non-HCC controls. Five of the 10 markers were newly found by CTTA and had not been previously identified as an HCC marker. We also analyzed the mutations and HBV integrations in the training cohort (tables S2 and S3) to set up the algorithm to detect HCC.

Last, an integrated model containing a panel of genetic and epigenetic biomarkers (panel E, table S1) was built for HCC detection. An algorithm that integrated the methylation score, yielded from the methylation model by random forest with default parameters, and the mutation score, defining as binary based on whether one or more reliable HCC-related mutations were detected, was developed. The combinational HCC detection model yielded an MCP score (fig. S7), taking the maximum of the mutation or methylation score. This HCC detection model had an area under the curve (AUC) of 0.96 [95% confidence interval (CI): 0.93 to 1.00] by leave-one-out cross-validation (Fig. 3A), with a sensitivity of 93% (56 of 60, 95% CI: 0.84 to 0.98) and a specificity of 95% (57 of 60, 95% CI: 0.86 to 0.99) for detecting HCC in the training cohort (Fig. 3, B and C).

Performance of the HCC detection model

Next, an independent cohort comprising 58 HCC cases and 198 non-HCC controls was used to validate the performance of the model for detecting HCC (tables S2 and S3). Our analysis showed that the model had a sensitivity of 90% (52 of 58, 95% CI: 0.79 to 0.96) and a specificity of 94% (187 of 198, 95% CI: 0.90 to 0.97) with an AUC of 0.93 (95% CI: 0.88 to 0.98) for detecting HCC cases (Fig. 3, B to D).

We also investigated the performance of the methylation and mutation biomarkers separately. In the methylation panel–based analysis, the methylation in HCC was different from non-HCC samples, as shown in the heatmap in Fig. 3E (data file S5). In the receiver operating characteristic (ROC) curve analysis based on the methylation score, the AUC value was 0.78 (95% CI: 0.70 to 0.87) in the validation cohort (Fig. 3D), and the sensitivity was 64% (37 of 58, 95% CI: 0.50 to 0.76) with a specificity of 95% (188 of 198, 95% CI: 0.91 to 0.98) (Fig. 3, B and C). The methylation score of cfDNA samples from patients with HCC were significantly higher than those from non-HCC individuals ($P < 0.0001$, one-tailed Mann-Whitney test; Fig. 3F). Furthermore, the methylation score increased with the tumor size (Fig. 3G). In the mutation panel, the mutation frequencies ranged from 0 to 17% among the HCC samples with multiple variant types across the mutation markers (Fig. 3E and tables S4 and S5). In the ROC curve analysis based on the mutation score, the AUC value was 0.79 (95% CI: 0.71 to 0.87) (Fig. 3D), with a sensitivity of 59% (34 of 58, 95% CI: 0.45 to 0.71) and a specificity of 99% (196 of 198, 95% CI: 0.96 to 1.00) for HCC detection (Fig. 3, B and C).

The performance of the HCC detection model was also analyzed at different stages of HCC. To do this, the training and validation cohorts were combined for ROC curve analysis. The analysis found AUC value of 0.88 (95% CI: 0.70 to 1.00) for stage 0, 0.95 (95% CI: 0.92 to 0.98) for stage A, 0.94 (95% CI: 0.87 to 1.00) for stage B, 0.99 (95% CI: 0.98 to 1.00) for stage C, and 0.95 (95% CI: 0.92 to 0.98) for all stages of HCC (Fig. 3H). The sensitivity was 86% (6 of 7, 95% CI: 0.42 to 1.00) for stage 0, 91% (72 of 79, 95% CI: 0.83 to 0.96) for stage A, 93% (26 of 28, 95% CI: 0.76 to 0.99) for stage B, 100% (4 of 4, 95% CI: 0.40 to 1.00) for stage C, and 92% (108 of 118, 95% CI: 0.85 to 0.96) for all stages, with a specificity of 95% (244 of 258, 95% CI: 0.91 to 0.97) (Fig. 3, B and I).

Combinational analysis of the mutation and methylation panels improves the performance of HCC detection

The AUC value of the combined mutation-methylation panel was greater than that of each panel alone in both the training (AUC: 0.96, 0.80, and 0.90 for MCP, mutation, and methylation, respectively) and validation (AUC: 0.93, 0.79, and 0.78 for MCP, mutation, and methylation, respectively) cohort for all HCC stages (Fig. 3, A and D). The sensitivity (93% for the training cohort and 90% for the validation cohort) of the combined mutation-methylation panel was higher than that of each panel alone (Fig. 3, C and J). Some cases that tested negative for HCC on the methylation panel tested positive on the mutation panel. Conversely, some cases that were missed by the mutation panel could be detected by the methylation panel (data file S5). Specifically, 24% (28 of 118) of the HCC cases were detected solely on the basis of mutation markers, and 31% (37 of 118) were detected solely on the basis of methylation markers. Only 36% (43 of 118) of the HCC cases showed positive prediction results according to both types of markers. This finding indicated that the parallel profiling of mutations and methylation markers could allow the detection of more HCC cases and improve the sensitivity of diagnosis.

We also compared the performance of the methylation, mutation, and combined mutation-methylation MCP profiling with the protein marker of alpha fetoprotein (AFP), the most commonly used blood-based biomarker for HCC (Fig. 3E). Fifty-five cases of the 118 patients with HCC in our study showed false-negative results with the AFP assay (<20 ng/ml), with sensitivity values of 43% (3 of 7, 95% CI: 0.10 to 0.82), 53% (42 to 79, 95% CI: 0.42 to 0.64), 61% (17 of 28, 95% CI: 0.41 to 0.78), 25% (1 of 4, 95% CI: 0.10 to 0.81), and 53% (63 of 118, 95% CI: 0.44 to 0.63) for HCC stages 0, A, B, and C, and all HCC stages, respectively. The performance of AFP was consistent to previous reports (*37*, *38*). These findings indicate that the HCC detection model based on our MCP technology outperforms AFP for the detection of HCC.

Comparison between mutation and methylation fractions in the same cfDNA sample

The parallel profiling feature of MCP enabled us to provide a direct comparison on the fraction of mutations and methylation changes in the same cfDNA sample, which have not been previously reported. We analyzed the correlation between the mutation fraction and the methylation fraction in individuals with positive signal of both methylation and mutation. The results showed that there was no significant correlation between the AFs of mutation and methylation ($r = 0.44$, $P = 3.7 \times 10^{-2}$; Fig. 4A). Our analysis showed that the methylation fraction was much higher than that of mutations (Fig. 4B). Among HCC cases with both methylation and mutation signals detected (Fig. 3E), the average methylation fraction was 37 (median, ranging from 2.6 to 1365.4) times higher than the average mutation fraction. Even the methylated fraction of some

Downloaded from https://www.science.org on November 25, 2022

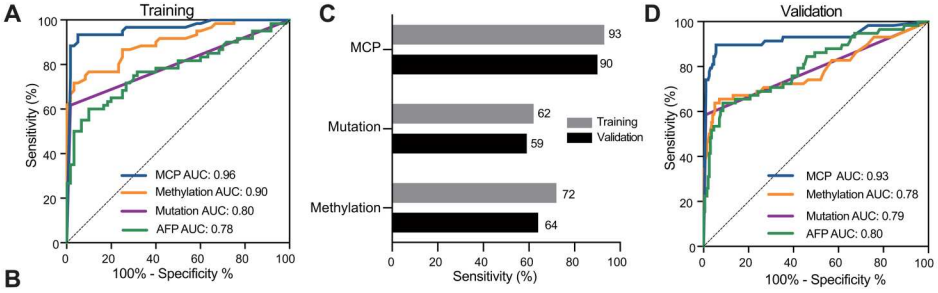

B

Performance of MCP in clinical plasma samples

		Methylation					Mutation				MCP			
		Total No.	Positive No.	Negative No.	Sensitivity % (95% CI)	Specificity % (95% CI)	Positive No.	Negative No.	Sensitivity % (95% CI)	Specificity % (95% CI)	Positive No.	Negative No.	Sensitivity % (95% CI)	Specificity % (95% CI)
Training	HCC	60	43	17	72 (59–83)	–	37	23	62 (48–74)	–	56	4	93 (84–98)	–
	Non-HCC	60	2	58	–	97 (88–100)	1	59	–	98 (91–100)	3	57	–	95 (86–99)
Validation	HCC	58	37	21	64 (50–76)	–	34	24	59 (45–71)	–	52	6	90 (79–96)	–
	Non-HCC	198	10	188	–	95 (91–98)	2	196	–	99 (96–100)	11	187	–	94 (90–97)
Total	Stage 0	7	2	5	29 (4–71)	–	5	2	71 (29–96)	–	6	1	86 (42–100)	–
	Stage A	79	52	27	66 (54–76)	–	48	31	61 (49–72)	–	72	7	91 (83–96)	–
	Stage B	28	22	6	79 (59–92)	–	15	13	54 (34–72)	–	26	2	93 (76–99)	–
	Stage C	4	4	0	100 (40–100)	–	3	1	75 (19–99)	–	4	0	100 (40–100)	–
	Non-HCC	258	12	246	–	95 (92–98)	3	255	–	99 (97–100)	14	244	–	95 (91–97)

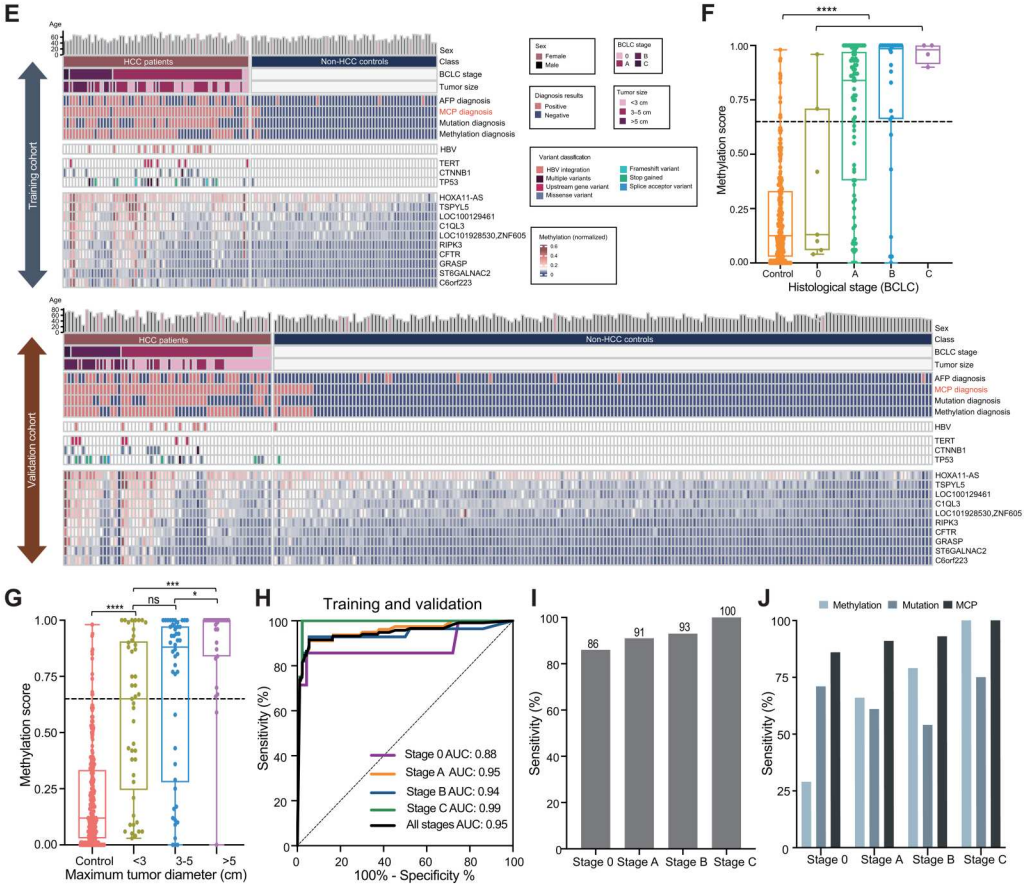

Fig. 3. Performance of the HCC detection model. (**A**) The ROC curves of different HCC diagnostic markers in the training cohort including MCP, methylation only, mutation only, and AFP, with AUC values showing in the figure. (**B**) Performance of the HCC detection model in clinical plasma samples. The performance (positive number, negative number, sensitivity, and specificity) of methylation only, mutation only, and MCP in detection of patients with HCC from training and testing cohort, as well as all patients with HCC at different stages. (**C**) Sensitivity of different groups of biomarkers in the detection of HCC. (**D**) The ROC curves of different HCC diagnostic markers in the validation cohort including MCP, methylation only, mutation only, and AFP, with AUC values showing in the figure. (**E**) Heatmap of the genetic and epigenetic alterations in clinical cfDNA samples in the training (top) and testing cohorts (bottom). Each column represents one cfDNA sample from one patient with HCC or non-HCC individual. Methylation and variant classification are shown in the heatmap. The diagnostic results of AFP, MCP, "Mutation," and "Methylation" are shown as positive (red) and negative (blue). BCLC, Barcelona Clinic Liver Cancer. (**F**) Methylation score of the 10 methylation markers in all patients with HCC at different stages and non-HCC control individuals. ****P < 0.0001. One-tailed Mann-Whitney test. (**G**) Methylation score of the 10 methylation markers in all patients with HCC with different tumor sizes and non-HCC control individuals. *P < 0.05; ***P < 0.005; ****P < 0.0001; ns, no significant difference. One-tailed Mann-Whitney test. (**H**) The ROC curve of the HCC detection panel at different stages. (**I**) Sensitivity of the HCC detection model at different stages of disease. (**J**) Sensitivity of different HCC detection panels in HCC at different stages.

methylation sites in non-HCC cfDNA samples could reach the fraction of >5%, which was higher than the fraction of most mutations in HCC cfDNA samples (Fig. 4C). These results suggested that there exists much higher noise of methylation than mutation in cfDNA samples, and some of the methylated cfDNA could be derived from nonneoplastic cells in the tumor, adjacent tissue, and normal tissues.

The performance of the HCC detection model in a prospective cohort

To test whether the assay can detect HCC before AFP and ultrasonography (US), we performed a pilot study by testing the HCC detection model in a prospective cohort. We applied the assay on the cfDNA samples of 311 surface antigen of HBV (HBsAg)–positive asymptomatic individuals who tested negative with AFP/US

Downloaded from https://www.science.org on November 25, 2022

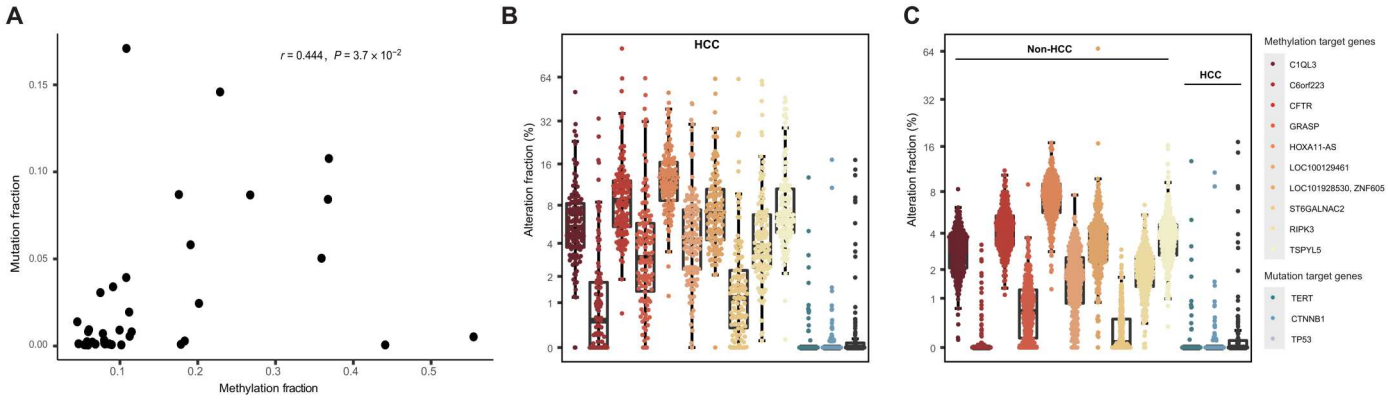

Fig. 4. Comparison between mutation and methylation fractions in the same cfDNA sample. (**A**) The correlation between the AF based on mutation and methylation. (**B**) Comparison of the alteration fraction between methylation changes and mutations in HCC. (**C**) Comparison of the methylation fraction in the non-HCC group with the mutation fraction in the HCC group. Each dot indicates one HCC or non-HCC sample. The *x* axis indicates methylation- and mutation-targeted genes. Here, methylation fraction was converted from the linear relationship between the actual methylation fraction in the standard references, and the methylation amount detected by MCP technology refers to the methylation detection assay in fig. S3C.

(tables S2 and S3). The HCC status was determined by follow-up visits with AFP/US and information from the local population–based cancer registry. The model detected four of five HCC cases in this cohort, showing 80% sensitivity (95% CI: 0.28 to 0.99), 94% specificity (95% CI: 0.91 to 0.96), and 18% positive predictive value (95% CI: 0.05 to 0.40) (Table 1).

DISCUSSION

Most noninvasive cancer detection studies focus on only one type of biomarker because the cfDNA yield is not sufficient to support multiple tests simultaneously. It is challenging to compare the performance of biomarkers profiled in different cohorts from different studies, making it difficult to combine biomarkers to develop a better algorithm for detecting cancer. In this study, we develop the MCP technology, which enables the multiplex testing of a single cfDNA sample without sacrificing sensitivity. The technology preserves and amplifies the information of mutations and methylation changes in a single pre-MCP library, which supports multiple tests of different downstream applications, including the genome-wide screening of previously unidentified methylation biomarkers, and parallel profiling of mutations and methylation changes. The multiplex test feature does not sacrifice sensitivity because the MCP profiling of the pre-MCP library is comparable to the direct profiling of the original cfDNA sample.

In addition, one advantage of MCP is that more original molecules can be detected through independent Watson or Crick strand amplification from two separate reactions, thus increasing the sensitivity of detecting mutations. The MCP technology showed strong performance for low-frequency mutations in low-yield cfDNA samples, in which MCP could achieve a sensitivity of 93.8 or 67.5% at 0.1% AF with 10 or 5 ng of input DNA, respectively. In comparison, a previously reported targeted digital sequencing method showed sensitivities of 50.8% at 0.125% AF with 7 to 8 ng of input DNA (*30*). In the detection of methylation, MCP could detect methylation sites at low frequency of 1%, which was comparable with the bisulfite-based methylation method. Here, MCP uses the method of methylation site–sensitive enzyme treatment, thereby avoiding template damage caused by bisulfite conversion.

In the current study, we also applied CTTA to pre-MCP libraries, which screened methylation markers for their potential as HCC biomarkers. The methylation markers found by this function covered multiple markers previously reported to be of diagnostic value in HCC, showing the reliability of the CTTA. Meanwhile, several new methylation markers were identified, which would help improve a cancer detection assay (*39*). We applied the MCP technology in the development of a liquid biopsy assay for HCC detection. We screened hypermethylated biomarkers that could distinguish HCC from non-HCC samples and selected 10 methylation markers by profiling the candidate markers in a training cohort. On the basis of genetic and epigenetic alterations, we established an HCC detection model and generated the algorithm to detect HCC. In an independent retrospective cohort, the model showed strong performance in the detection of HCC. The cfDNA-based assay was superior to AFP analysis, either at the commonly used cutoff of 20 ng/ml or at the Youden index–based cutoff of 14.8 ng/ml by ROC analysis. The genetic mutations and methylation changes showed complementary patterns among the HCC

Downloaded from https://www.science.org on November 25, 2022

Table 1. Performance of the HCC detection model in the prospective cohort.

	Total number	Predicated HCC	Predicated non-HCC	Sensitivity (%)	Specificity (%)
	No.	No.	No.	% (95% CI)	% (95% CI)
True HCC	5	4	1	80 (28–99)	
True non-HCC	306	18	288		94 (91–96)

cases, and parallel profiling improved sensitivity in the detection of HCC. This is similar to other reports that the combination of mutations and methylation markers leads to better performance in the early screening of colorectal cancer from stool samples (*10*).

The model was validated in a prospective cohort with promising performance by detecting HCC cases that were missed by AFP/US. We were able to evaluate the HCC detection model for the ability to be used as an early screening tool for HCC from high-risk individuals, as well as evaluating its use for differential diagnosis, which was validated in a retrospective cohort.

However, there still exist some limitations of this study. Because our MCP technology is an enzyme-dependent method in methylation detection, only methylation changes in GCGC cleavage site could be detected, which means that it cannot profile methylation in single-base resolution. Second, MCP cannot distinguish 5- methylcytosine (5mc) from 5-hydroxymethylcytosine (5hmc) because Hha I cannot digest the cfDNA with either of these two epigenetic modifications. For the detection of mutation, there are three GCGC restriction sites concentrated in the coding region of TP53, leading to a 71-bp region (6% of the TP53-coding regions) unavailable for mutation profiling. In addition, our prospective cohort is only a pilot study, the sample size and the number of HCC cases are relatively limited, and further work in clinical trial with a larger cohort would be necessary to fully validate the performance in the early detection of HCC. It is also worth mentioning that our HCC detection model could be more suitable for HCC screening in HBV-infected high-risk population, and the performance in population with other risk factors like hepatitis C virus infection needs to be validated in future studies.

In summary, we developed a technology supporting multiplex testing of a single cfDNA sample for the discovery or profiling of methylation changes in parallel with mutations. The MCP technology was able to help develop a liquid biopsy assay for HCC with robust performance, as compared to other assays currently in use or the evaluation of either methylation or mutation markers alone. The technology and strategy, including identification of new methylation markers and combined profiling of mutation and methylation, could be applied to develop liquid biopsy assays for other tumor types. Because of the multiplex testing feature, the pre-MCP libraries in one study could be used in future studies to profile different panels of biomarkers for other tumor types or multiple tumor types.

MATERIALS AND METHODS

Study design

The aim of this study was to develop a cfDNA profiling technology to help in discovery and validation of multiomics biomarkers for the noninvasive detection of cancer. We developed MCP technology, which preserved and amplified the information of mutations and methylation changes in a single pre-MCP library and supported multiple tests of different downstream applications, including the genome-wide screening of new methylation biomarkers, and parallel profiling of mutations and methylation changes. The analytical performance of MCP was demonstrated in commercially available reference samples with known mutation and methylation fractions. We then aimed to apply the MCP technology to a discovery, training, and validation cohort of a liquid biopsy assay for the detection of HCC. First, we performed de novo screening of methylation markers on cfDNA samples from HCC cases and non-HCC controls. The methylation markers enriched in HCC cfDNA were further profiled in parallel with a panel of mutations on a training cohort, resulting in an HCC detection model. We then validated the model in an independent retrospective cohort with HCC cases and non-HCC controls. Furthermore, we validated the potential value of this HCC detection model in the blood samples from a prospective cohort of asymptomatic HBsAg-positive individuals with normal AFP/US. Prior power analysis, randomization, or blinding was not performed for this study.

Patients and blood sample collection

The study protocol for blood sample collection was approved by the Institutional Review Board of the National Cancer Center, Chinese Academy of Medical Sciences. The study was approved by the Ethics Committee of the National Cancer Center (Ethics no.17-162/1418). All the participants signed written informed consent forms for the collection of samples and subsequent analyses before their inclusion in the study. Blood samples of HCC were obtained at the time of diagnosis, before tumor resection or any other treatment. Blood samples of non-HCC were obtained from HBsAg-positive individuals who were free of HCC. Individuals with a previous malignancy within the past 5 years were excluded. In total, 148 blood samples from patients with HCC and 288 from HBV-infected non-HCC individuals were collected. Thirty HCC and 30 non-HCC samples were used in de novo methylation marker discovery. The remaining samples were divided into training (60 HCC and 60 non-HCC) and validation (58 HCC and 198 non-HCC) cohorts for the development and validation of the HCC detection model. The clinical and sequencing data are summarized in tables S2 and S3, respectively.

For the prospective validation, baseline blood samples were collected from 311 HBsAg-positive asymptomatic individuals who took AFP/US screening and showed normal liver US and serum AFP concentration (<20 ng/ml). Follow-up visits with AFP/US tests were provided every 6 months for at least 12 months. All suspected individuals (AFP concentration ≧20 ng/ml or US-detected nodule ≧1 cm in size) in the follow-up visits were further diagnosed with dynamic computed tomography/magnetic resonance imaging, and all patients with confirmed HCC received relevant therapy based on clinical practice guidelines. The HCC status was also obtained from local population–based cancer registry. Together, we determined the HCC status of the 311 participants and identified 5 HCC cases out of the 311 individuals. The mutation and methylation statuses of the baseline cfDNA samples were profiled by the MCP-based assay and evaluated with the HCC detection model. The outcome of the HCC detection model was compared with the HCC status to determine the sensitivity and specificity of the assay. The clinical and sequencing data are summarized in tables S2 and S3, respectively.

DNA extraction

cfDNA was extracted from the plasma samples using the Apostle MiniMax cfDNA isolation kit (C43468, Apostle). WBC DNA was extracted using the QIAamp DNA mini kit (51306, Qiagen). DNA concentrations were determined using the Qubit dsDNA HS Assay Kit (Q32854, Thermo Fisher Scientific).

Downloaded from https://www.science.org on November 25, 2022

Construction of pre-MCP library

Fragmented DNA (see the Supplementary Materials) and cfDNA (5 to 100 ng) were digested with the methylation-sensitive restriction enzyme Hha I (R0139L, New England BioLabs) at 37°C for 30 min and 65°C for 20 min. The libraries were prepared using the UltraII DNA library prep kit (E7370L, New England Biolabs) according to the manufacturer's protocols. Specifically, (i) the digested cfDNA was treated with end repair and A-tailing, (ii) the cfDNA ligated to customized MCP adapters containing DNA barcode for UID (fig. S2 and table S6), and (iii) the ligation product was amplified for 9 cycles with the KAPA HiFi PCR kit (KR0369, Kapa Biosystems) with customized amplification primers. The cycling conditions were as follows: 98°C for 45 s; 9 cycles of 98°C for 15 s, 60°C for 30 s, and 72°C for 30 s; 72°C for 5 min.

Targeted amplification and construction of MCP library

First, the pre-MCP library was digested using lambda exonuclease (M0262L, New England Biolabs) to remove the strands with phosphate modification. The digestion reaction was prepared in a 20-μl volume containing 2 μl of the 10× reaction buffer, 1 μl of lambda exonuclease, and 17 μl of the pre-MCP library (400 ng) and was incubated at 37°C for 10 min and 75°C for 10 min. After digestion, the single-stranded DNA was equally divided into two aliquots and amplified using a two-step PCR (fig. S1). In the first step, a linear amplification was performed in a 30-μl reaction containing 1× Platinum PCR Master Mix (14000012, Thermo Fisher Scientific) and MCP primer pool 1A or primer pool 1B (0.01 μM each; see table S1 for the primer sequences in different panels) under the following cycling conditions: 98°C for 3 min; 20 cycles of 98°C for 15 s, 60°C for 90 s, and 72°C for 90 s; and a final step of 72°C for 5 min. The products were purified using AMPure XP beads (A63882, Beckman Coulter) and diluted in 20 μl of nuclease-free water. In the second step, 10 μl of the purified product from step 1 was amplified with universal primers and MCP primer pool 2A or primer pool 2B (see table S1 for the primer sequences in different panels). Index sequences and sequences for full-length adapters of Illumina sequencing were also added in this step. The amplification reaction was prepared in a 30-μl volume reaction containing 1× Platinum PCR Master Mix and run under the following cycling conditions: 98°C for 3 min; 8 cycles of 98°C for 15 s, 60°C for 90 s, and 72°C for 90 s; and 6 cycles of 98°C for 15 s, 60°C for 30 s, and 72°C for 30 s. Last, the PCR product of the two pools were combined and purified using AMPure XP beads. The final library was sequenced on the Illumina NovaSeq 6000 platform (Illumina).

CpG tandems target amplification

CTTA was used for the discovery of methylation markers from the pre-MCP library. After lambda exonuclease digestion, the single-stranded DNA was equally divided into two aliquots, followed by two-step PCR amplification. In the first step, a linear amplification reaction was prepared in a 30-μl volume containing 1× Platinum PCR Master Mix (14000012, Thermo Fisher Scientific) and CTT primer pool A or primer pool B (0.07 μM for each primer, panel D, table S1) under the following cycling conditions: 98°C for 3 min, followed by 3 cycles of 98°C for 15 s, 51°C for 240 s, 68°C for 90 s, and 72°C for 5 min. Then, the PCR products using the two pools were combined, purified using AMPure XP beads (A63882, Beckman Coulter), and diluted in 20 μl of ddH_2O. In the second step, the 20 μl of purified product from step 1 was amplified with index primers in a 50-μl of reaction containing 1× KAPA HiFi HotStart ReadyMix (KR0369, Kapa Biosystems), followed by PCR under the following conditions: 98°C for 45 s; 13 cycles of 98°C for 15 s, 62°C for 30 s, and 72°C for 30 s; and 72°C for 5 min. Last, the PCR product was purified and sequenced on the Illumina NovaSeq 6000 platform (Illumina).

Construction of the diagnostic model for HCC detection

Ten methylation markers with diagnostic value were identified on a training cohort comprising HCC and non-HCC samples by random forest algorithm. Then, these 10 methylation markers were used for methylation model by random forest with default parameters, yielding the methylation score. The mutation score was defined as binary based on whether one or more reliable HCC-related mutations were detected. The final HCC detection model contained the combined mutation and methylation score based on taking the maximum of each of the mutation or methylation score, as the MCP score. The model performance was evaluated both on the training and testing cohorts by the AUC statistics. Sensitivity and specificity of the model was determined using an optimized cutoff value of 0.63, generated from the training cohort with leave-one-out cross-validation algorithm. This cutoff value optimization was applied using Youden's index.

Statistical analysis

Custom R script and R packages software was used to construct heatmap and boxplot and to perform statistical analysis. The analysis scripts are available at Zenodo (DOI:10.5281/zenodo.7106903). GraphPad Prism (PRISM version 5) software was used to construct bar plots, correlation analysis graph, and ROC curve analysis. The correlations between the observed and expected frequencies in reference samples and between different mutation or methylation detection methods were evaluated using Spearman correlation coefficients. The statistical significance of the difference was determined using the Wilcoxon signed-rank test or one-tailed Mann-Whitney test. The 95% CIs for sensitivity and specificity in HCC detection were estimated by the Clopper-Pearson method.

Supplementary Materials

This PDF file includes:
Methods
Figs. S1 to S7
References (*40*–*54*)

Other Supplementary Material for this manuscript includes the following:
Tables S1 to S6
Data files S1 to S5
MDAR Reproducibility Checklist

View/request a protocol for this paper from *Bio-protocol*.

REFERENCES AND NOTES

1. H. Sung, J. Ferlay, R. L. Siegel, M. Laversanne, I. Soerjomataram, A. Jemal, F. Bray, Global cancer statistics 2020: GLOBOCAN estimates of incidence and mortality worldwide for 36 cancers in 185 countries. *CA Cancer J. Clin.* **71**, 209–249 (2021).
2. M. Omata, A.-L. Cheng, N. Kokudo, M. Kudo, J. M. Lee, J. Jia, R. Tateishi, K.-H. Han, Y. K. Chawla, S. Shiina, Asia–Pacific clinical practice guidelines on the management of hepatocellular carcinoma: A 2017 update. *Hepatol. Int.* **11**, 317–370 (2017).

Downloaded from https://www.science.org on November 25, 2022

3. J. A. Marrero, L. M. Kulik, C. B. Sirlin, A. X. Zhu, R. S. Finn, M. M. Abecassis, L. R. Roberts, J. K. Heimbach, Diagnosis, staging, and management of hepatocellular carcinoma: 2018 practice guidance by the American Association for the Study of Liver Diseases. *Hepatology* **68**, 723–750 (2018).
4. A. G. Singal, A. Pillai, J. Tiro, Early detection, curative treatment, and survival rates for hepatocellular carcinoma surveillance in patients with cirrhosis: A meta-analysis. *PLOS Med.* **11**, e1001624 (2014).
5. C. Bettegowda, M. Sausen, R. J. Leary, I. Kinde, Y. Wang, N. Agrawal, B. R. Bartlett, H. Wang, B. Luber, R. M. Alani, E. S. Antonarakis, N. S. Azad, A. Bardelli, H. Brem, J. L. Cameron, C. C. Lee, L. A. Fecher, G. L. Gallia, P. Gibbs, D. Le, R. L. Giuntoli, M. Goggins, M. D. Hogarty, M. Holdhoff, S.-M. Hong, Y. Jiao, H. H. Juhl, J. J. Kim, G. Siravegna, D. A. Laheru, C. Lauricella, M. Lim, E. J. Lipson, S. K. Nagahashi Marie, G. J. Netto, K. S. Oliner, A. Olivi, L. Olsson, G. J. Riggins, A. Sartore-Bianchi, K. Schmidt, L.-M. Shih, S. M. Oba-Shinjo, S. Siena, D. Theodorescu, J. Tie, T. T. Harkins, S. Veronese, T.-L. Wang, J. D. Weingart, C. L. Wolfgang, L. D. Wood, D. Xing, R. H. Hruban, J. Wu, P. J. Allen, C. M. Schmidt, M. A. Choti, V. E. Velculescu, K. W. Kinzler, B. Vogelstein, N. Papadopoulos, L. A. Diaz Jr., Detection of circulating tumor DNA in early-and late-stage human malignancies. *Sci. Transl. Med.* **6**, 224ra24 (2014).
6. A. A. Chaudhuri, J. J. Chabon, A. F. Lovejoy, A. M. Newman, H. Stehr, T. D. Azad, M. S. Khodadoust, M. S. Esfahani, C. L. Liu, L. Zhou, F. Scherer, D. M. Kurtz, C. Say, J. N. Carter, D. J. Merriott, J. C. Dudley, M. S. Binkley, L. Modlin, S. K. Padda, M. F. Gensheimer, R. B. West, J. B. Shrager, J. W. Neal, H. A. Wakelee, B. W. Loo Jr., A. A. Alizadeh, M. Diehn, Early detection of molecular residual disease in localized lung cancer by circulating tumor DNA profiling. *Cancer Discov.* **7**, 1394–1403 (2017).
7. J. D. Cohen, L. Li, Y. Wang, C. Thoburn, B. Afsari, L. Danilova, C. Douville, A. A. Javed, F. Wong, A. Mattox, R. H. Hruban, C. L. Wolfgang, M. G. Goggins, M. D. Molin, T.-L. Wang, R. Roden, A. P. Klein, J. Ptak, L. Dobbyn, J. Schaefer, N. Silliman, M. Popoli, J. T. Vogelstein, J. D. Browne, R. E. Schoen, R. E. Brand, J. Tie, P. Gibbs, H.-L. Wong, A. S. Mansfield, J. Jen, S. M. Hanash, M. Falconi, P. J. Allen, S. Zhou, C. Bettegowda, L. A. Diaz Jr., C. Tomasetti, K. W. Kinzler, B. Vogelstein, A. M. Lennon, N. Papadopoulos, Detection and localization of surgically resectable cancers with a multi-analyte blood test. *Science* **359**, 926–930 (2018).
8. R.-h. Xu, W. Wei, M. Krawczyk, W. Wang, H. Luo, K. Flagg, S. Yi, W. Shi, Q. Quan, K. Li, K. Li, L. Zheng, H. Zhang, B. A. Caughey, Q. Zhao, J. Hou, R. Zhang, Y. Xu, H. Cai, G. Li, R. Hou, Z. Zhong, D. Lin, X. Fu, J. Zhu, Y. Duan, M. Yu, B. Ying, W. Zhang, J. Wang, E. Zhang, C. Zhang, O. Li, R. Guo, H. Carter, J.-k. Zhu, X. Hao, K. Zhang, Circulating tumour DNA methylation markers for diagnosis and prognosis of hepatocellular carcinoma. *Nat. Mater.* **16**, 1155–1161 (2017).
9. H. Luo, Q. Zhao, W. Wei, L. Zheng, S. Yi, G. Li, W. Wang, H. Sheng, H. Pu, H. Mo, Z. Zuo, Z. Liu, C. Li, C. Xie, Z. Zeng, W. Li, X. Hao, Y. Liu, S. Cao, W. Liu, S. Gibson, K. Zhang, G. Xu, R.-H. Xu, Circulating tumor DNA methylation profiles enable early diagnosis, prognosis prediction, and screening for colorectal cancer. *Sci. Transl. Med.* **12**, eaax7533 (2020).
10. T. F. Imperiale, D. F. Ransohoff, S. H. Itzkowitz, T. R. Levin, P. Lavin, G. P. Lidgard, D. A. Ahlquist, B. M. Berger, Multitarget stool DNA testing for colorectal-cancer screening. *N. Engl. J. Med.* **370**, 1287–1297 (2014).
11. M. C. Liu, G. R. Oxnard, E. A. Klein, C. Swanton, M. V. Seiden; CCGA Consortium, Sensitive and specific multi-cancer detection and localization using methylation signatures in cell-free DNA. *Ann. Oncol.* **31**, 745–759 (2020).
12. Z. Zheng, M. Liebers, B. Zhelyazkova, Y. Cao, D. Panditi, K. D. Lynch, J. Chen, H. E. Robinson, H. S. Shim, J. Chmielecki, W. Pao, J. A. Engelman, A. J. Iafrate, L. P. Le, Anchored multiplex PCR for targeted next-generation sequencing. *Nat. Med.* **20**, 1479–1484 (2014).
13. M. W. Schmitt, S. R. Kennedy, J. J. Salk, E. J. Fox, J. B. Hiatt, L. A. Loeb, Detection of ultra-rare mutations by next-generation sequencing. *Proc. Natl. Acad. Sci.* **109**, 14508–14513 (2012).
14. C. Qu, Y. Wang, P. Wang, K. Chen, M. Wang, H. Zeng, J. Lu, Q. Song, B. H. Diplas, D. Tan, C. Fan, Q. Guo, Z. Zhu, H. Yin, L. Jiang, X. Chen, H. Zhao, H. He, Y. Wang, G. Li, X. Bi, X. Zhao, T. Chen, H. Tang, C. Lv, D. Wang, W. Chen, J. Zhou, H. Zhao, J. Cai, X. Wang, S. Wang, H. Yan, Y.-X. Zeng, W. K. Cavenee, Y. Jiao, Detection of early-stage hepatocellular carcinoma in asymptomatic HBsAg-seropositive individuals by liquid biopsy. *Proc. Natl. Acad. Sci. U.S.A.* **116**, 6308–6312 (2019).
15. K. Szymańska, O. A. Lesi, G. D. Kirk, O. Sam, P. Taniere, J. Y. Scoazec, M. Mendy, M. D. Friesen, H. Whittle, R. Montesano, P. Hainaut, Ser-249TP53 mutation in tumour and plasma DNA of hepatocellular carcinoma patients from a high incidence area in the Gambia, West Africa. *Int. J. Cancer* **110**, 374–379 (2004).
16. A. Huang, X. Zhao, X.-R. Yang, F.-Q. Li, X.-L. Zhou, K. Wu, X. Zhang, Q.-M. Sun, Y. Cao, H.-M. Zhu, X.-D. Wang, H.-M. Yang, J. Wang, Z.-Y. Tang, Y. Hou, J. Fan, J. Zhou, Circumventing intratumoral heterogeneity to identify potential therapeutic targets in hepatocellular carcinoma. *J. Hepatol.* **67**, 293–301 (2017).
17. C. Ng, G. Di Costanzo, N. Tosti, V. Paradiso, M. Coto-Llerena, G. Roscigno, V. Perrina, C. Quintavalle, T. Boldanova, S. Wieland, G. Marino-Marsilia, M. Lanzafame, L. Quagliata, G. Condorelli, M. S. Matter, R. Tortora, M. H. Heim, L. M. Terracciano, S. Piscuoglio, Genetic profiling using plasma-derived cell-free DNA in therapy-naïve hepatocellular carcinoma patients: A pilot study. *Ann. Oncol.* **29**, 1286–1291 (2018).
18. I. Labgaa, C. Villacorta-Martin, D. D'Avola, A. J. Craig, J. von Felden, S. N. Martins-Filho, D. Sia, A. Stueck, S. C. Ward, M. I. Fiel, M. Mahajan, P. Tabrizian, S. N. Thung, C. Ang, S. L. Friedman, J. M. Llovet, M. Schwartz, A. Villanueva, A pilot study of ultra-deep targeted sequencing of plasma DNA identifies driver mutations in hepatocellular carcinoma. *Oncogene* **37**, 3740–3752 (2018).
19. J. Howell, S. R. Atkinson, D. J. Pinato, S. Knapp, C. Ward, R. Minisini, M. E. Burlone, M. Leutner, M. Pirisi, R. Büttner, S. A. Khan, M. Thursz, M. Odenthal, R. Sharma, Identification of mutations in circulating cell-free tumour DNA as a biomarker in hepatocellular carcinoma. *Eur. J. Cancer* **116**, 56–66 (2019).
20. A. M. Aravanis, M. Lee, R. D. Klausner, Next-generation sequencing of circulating tumor DNA for early cancer detection. *Cell* **168**, 571–574 (2017).
21. S. B. Baylin, P. A. Jones, A decade of exploring the cancer epigenome—Biological and translational implications. *Nat. Rev. Cancer* **11**, 726–734 (2011).
22. M. A. Dawson, The cancer epigenome: Concepts, challenges, and therapeutic opportunities. *Science* **355**, 1147–1152 (2017).
23. J.-P. Issa, CpG island methylator phenotype in cancer. *Nat. Rev. Cancer* **4**, 988–993 (2004).
24. H. Schwarzenbach, D. S. Hoon, K. Pantel, Cell-free nucleic acids as biomarkers in cancer patients. *Nat. Rev. Cancer* **11**, 426–437 (2011).
25. H. Wu, X. Wu, L. Shen, Y. Zhang, Single-base resolution analysis of active DNA demethylation using methylase-assisted bisulfite sequencing. *Nat. Biotechnol.* **32**, 1231–1240 (2014).
26. K. Tanaka, A. Okamoto, Degradation of DNA by bisulfite treatment. *Bioorg. Med. Chem. Lett.* **17**, 1912–1915 (2007).
27. S. Springer, Y. Wang, M. Dal Molin, D. L. Masica, Y. Jiao, I. Kinde, A. Blackford, S. P. Raman, C. L. Wolfgang, T. Tomita, N. Niknafs, C. Douville, J. Ptak, L. Dobbyn, P. J. Allen, D. S. Klimstra, M. A. Schattner, C. M. Schmidt, M. Yip-Schneider, O. W. Cummings, R. E. Brand, H. J. Zeh, A. D. Singhi, A. Scarpa, R. Salvia, G. Malleo, G. Zamboni, M. Falconi, J.-Y. Jang, S.-W. Kim, W. Kwon, S.-M. Hong, K.-B. Song, S. C. Kim, N. Swan, J. Murphy, J. Geoghegan, W. Brugge, C. Fernandez-Del Castillo, M. Mino-Kenudson, R. Schulick, B. H. Edil, V. Adsay, J. Paulino, J. van Hooft, S. Yachida, S. Nara, N. Hiraoka, K. Yamao, S. Hijioka, S. van der Merwe, M. Goggins, M. I. Canto, N. Ahuja, K. Hirose, M. Makary, M. J. Weiss, J. Cameron, M. Pittman, J. R. Eshleman, L. A. Diaz Jr., N. Papadopoulos, K. W. Kinzler, R. Karchin, R. H. Hruban, B. Vogelstein, A. M. Lennon, A combination of molecular markers and clinical features improve the classification of pancreatic cysts. *Gastroenterology* **149**, 1501–1510 (2015).
28. S. R. Kennedy, M. W. Schmitt, E. J. Fox, B. F. Kohrn, J. J. Salk, E. H. Ahn, M. J. Prindle, K. J. Kuong, J.-C. Shen, R.-A. Risques, L. A. Loeb, Detecting ultralow-frequency mutations by duplex sequencing. *Nat. Protoc.* **9**, 2586–2606 (2014).
29. M. T. Gregory, J. A. Bertout, N. G. Ericson, S. D. Taylor, R. Mukherjee, H. S. Robins, C. W. Drescher, J. H. Bielas, Targeted single molecule mutation detection with massively parallel sequencing. *Nucleic Acids Res.* **44**, e22 (2016).
30. B. R. McDonald, T. Contente-Cuomo, S.-J. Sammut, A. Odenheimer-Bergman, B. Ernst, N. Perdigones, S.-F. Chin, M. Farooq, R. Mejia, P. A. Cronin, Personalized circulating tumor DNA analysis to detect residual disease after neoadjuvant therapy in breast cancer. *Sci. Transl. Med.* **11**, eaax7392 (2019).
31. J. B. Kisiel, B. A. Dukek, R. V. S. R. Kanipakam, H. M. Ghoz, T. C. Yab, C. K. Berger, W. R. Taylor, P. H. Foote, N. H. Giama, K. Onyirioha, Hepatocellular carcinoma detection by plasma methylated DNA: Discovery, phase I pilot, and phase II clinical validation. *Hepatology* **69**, 1180–1192 (2019).
32. L. Wen, J. Li, H. Guo, X. Liu, S. Zheng, D. Zhang, W. Zhu, J. Qu, L. Guo, D. Du, X. Jin, Y. Zhang, Y. Gao, J. Shen, H. Ge, F. Tang, Y. Huang, J. Peng, Genome-scale detection of hypermethylated CpG islands in circulating cell-free DNA of hepatocellular carcinoma patients. *Cell Res.* **25**, 1250–1264 (2015).
33. Y. Totoki, K. Tatsuno, K. R. Covington, H. Ueda, C. J. Creighton, M. Kato, S. Tsuji, L. A. Donehower, B. L. Slagle, H. Nakamura, S. Yamamoto, E. Shinbrot, N. Hama, M. Lehmkuhl, F. Hosoda, Y. Arai, K. Walker, M. Dahdouli, K. Gotoh, G. Nagae, M.-C. Gingras, D. M. Muzny, H. Ojima, K. Shimada, Y. Midorikawa, J. A. Goss, R. Cotton, A. Hayashi, J. Shibahara, S. Ishikawa, J. Guiteau, M. Tanaka, T. Urushidate, S. Ohashi, N. Okada, H. Doddapaneni, M. Wang, Y. Zhu, H. Dinh, T. Okusaka, N. Kokudo, T. Kosuge, T. Takayama, M. Fukayama, R. A. Gibbs, D. A. Wheeler, H. Aburatani, T. Shibata, Trans-ancestry mutational landscape of hepatocellular carcinoma genomes. *Nat. Genet.* **46**, 1267–1273 (2014).
34. W. Zhang, H. He, M. Zang, Q. Wu, H. Zhao, L.-l. Lu, P. Ma, H. Zheng, N. Wang, Y. Zhang, S. He, X. Chen, Z. Wu, X. Wang, J. Cai, Z. Liu, Z. Sun, Y.-X. Zeng, C. Qu, Y. Jiao, Genetic features of aflatoxin-associated hepatocellular carcinoma. *Gastroenterology* **153**, 249–262.e2 (2017).
35. J. Cheng, D. Wei, Y. Ji, L. Chen, L. Yang, G. Li, L. Wu, T. Hou, L. Xie, G. Ding, H. Li, Y. Li, Integrative analysis of DNA methylation and gene expression reveals hepatocellular carcinoma-specific diagnostic biomarkers. *Genome Med.* **10**, 42 (2018).

Downloaded from https://www.science.org on November 25, 2022

36. Y. Zheng, Q. Huang, Z. Ding, T. Liu, C. Xue, X. Sang, J. Gu, Genome-wide DNA methylation analysis identifies candidate epigenetic markers and drivers of hepatocellular carcinoma. *Brief. Bioinform.* **19**, 101–108 (2018).
37. P. Stefaniuk, J. Cianciara, A. Wiercinska-Drapalo, Present and future possibilities for early diagnosis of hepatocellular carcinoma. *World J Gastroenterol: WJG* **16**, 418–424 (2010).
38. J. Bruix, M. Sherman; American Association for the Study of Liver Diseases, Management of hepatocellular carcinoma: An update. *Hepatology* **53**, 1020–1022 (2011).
39. S. S. Hori, S. S. Gambhir, Mathematical model identifies blood biomarker–based early cancer detection strategies and limitations. *Sci. Transl. Med.* **3**, 109ra116 (2011).
40. A. McKenna, M. Hanna, E. Banks, A. Sivachenko, K. Cibulskis, A. Kernytsky, K. Garimella, D. Altshuler, S. Gabriel, M. Daly, M. A. DePristo, The Genome Analysis Toolkit: A MapReduce framework for analyzing next-generation DNA sequencing data. *Genome Res.* **20**, 1297–1303 (2010).
41. S. Jaiswal, P. Natarajan, A. J. Silver, C. J. Gibson, A. G. Bick, E. Shvartz, M. McConkey, N. Gupta, S. Gabriel, D. Ardissino, U. Baber, R. Mehran, V. Fuster, J. Danesh, P. Frossard, D. Saleheen, O. Melander, G. K. Sukhova, D. Neuberg, P. Libby, S. Kathiresan, B. L. Ebert, Clonal hematopoiesis and risk of atherosclerotic cardiovascular disease. *N. Engl. J. Med.* **377**, 111–121 (2017).
42. C. C. Coombs, A. Zehir, S. M. Devlin, A. Kishtagari, A. Syed, P. Jonsson, D. M. Hyman, D. B. Solit, M. E. Robson, J. Baselga, M. E. Arcila, M. Ladanyi, M. S. Tallman, R. L. Levine, M. F. Berger, Therapy-related clonal hematopoiesis in patients with non-hematologic cancers is common and associated with adverse clinical outcomes. *Cell Stem Cell* **21**, 374–382.e4 (2017).
43. Z. Li, W. Huang, J. C. Yin, C. Na, X. Wu, Y. Shao, H. Ding, J. Li, Comprehensive next-generation profiling of clonal hematopoiesis in cancer patients using paired tumor-blood sequencing for guiding personalized therapies. *Clin. Transl. Med.* **10**, e222 (2020).
44. R. N. Ptashkin, D. L. Mandelker, C. C. Coombs, K. Bolton, Z. Yelskaya, D. M. Hyman, D. B. Solit, J. Baselga, M. E. Arcila, M. Ladanyi, L. Zhang, R. L. Levine, M. F. Berger, A. Zehir, Prevalence of clonal hematopoiesis mutations in tumor-only clinical genomic profiling of solid tumors. *JAMA Oncol.* **4**, 1589–1593 (2018).
45. P. Razavi, B. T. Li, D. N. Brown, B. Jung, E. Hubbell, R. Shen, W. Abida, K. Juluru, I. De Bruijn, C. Hou, O. Venn, R. Lim, A. Anand, T. Maddala, S. Gnerre, R. V. Satya, Q. Liu, L. Shen, N. Eattock, J. Yue, A. W. Blocker, M. Lee, A. Sehnert, H. Xu, M. P. Hall, A. Santiago-Zayas, W. F. Novotny, J. M. Isbell, V. W. Rusch, G. Plitas, A. S. Heerdt, M. Ladanyi, D. M. Hyman, D. R. Jones, M. Morrow, G. J. Riely, H. I. Scher, C. M. Rudin, M. E. Robson, L. A. Diaz Jr., D. B. Solit, A. M. Aravanis, J. S. Reis-Filho, High-intensity sequencing reveals the sources of plasma circulating cell-free DNA variants. *Nat. Med.* **25**, 1928–1937 (2019).
46. Y. Zhang, Y. Yao, Y. Xu, L. Li, Y. Gong, K. Zhang, M. Zhang, Y. Guan, L. Chang, X. Xia, Pan-cancer circulating tumor DNA detection in over 10,000 Chinese patients. *Nat. Commun.* **12**, 11 (2021).
47. J. Xia, C. A. Miller, J. Baty, A. Ramesh, M. R. Jotte, R. S. Fulton, T. P. Vogel, M. A. Cooper, K. J. Walkovich, V. Makaryan, A. A. Bolyard, M. C. Dinauer, D. B. Wilson, A. Vlachos, K. C. Myers, R. J. Rothbaum, A. A. Bertuch, D. C. Dale, A. Shimamura, L. A. Boxer, D. C. Link, Somatic mutations and clonal hematopoiesis in congenital neutropenia. *Blood* **131**, 408–416 (2018).
48. S. Jaiswal, P. Fontanillas, J. Flannick, A. Manning, P. V. Grauman, B. G. Mar, R. C. Lindsley, C. H. Mermel, N. Burtt, A. Chavez, J. M. Higgins, V. Moltchanov, F. C. Kuo, M. J. Kluk, B. Henderson, L. Kinnunen, H. A. Koistinen, C. Ladenvall, G. Getz, A. Correa, B. F. Banahan, S. Gabriel, S. Kathiresan, H. M. Stringham, M. I. McCarthy, M. Boehnke, J. Tuomilehto, C. Haiman, L. Groop, G. Atzmon, J. G. Wilson, D. Neuberg, D. Altshuler, B. L. Ebert, Age-related clonal hematopoiesis associated with adverse outcomes. *N. Engl. J. Med.* **371**, 2488–2498 (2014).
49. G. Genovese, A. K. Kähler, R. E. Handsaker, J. Lindberg, S. A. Rose, S. F. Bakhoum, K. Chambert, E. Mick, B. M. Neale, M. Fromer, S. M. Purcell, O. Svantesson, M. Landén, M. Höglund, S. Lehmann, S. B. Gabriel, J. L. Moran, E. S. Lander, P. F. Sullivan, P. Sklar, H. Grönberg, C. M. Hultman, S. A. McCarroll, Clonal hematopoiesis and blood-cancer risk inferred from blood DNA sequence. *N. Engl. J. Med.* **371**, 2477–2487 (2014).
50. M. Xie, C. Lu, J. Wang, M. D. McLellan, K. J. Johnson, M. C. Wendl, J. F. McMichael, H. K. Schmidt, V. Yellapantula, C. A. Miller, B. A. Ozenberger, J. S. Welch, D. C. Link, M. J. Walter, E. R. Mardis, J. F. Dipersio, F. Chen, R. K. Wilson, T. J. Ley, L. Ding, Age-related mutations associated with clonal hematopoietic expansion and malignancies. *Nat. Med.* **20**, 1472–1478 (2014).
51. H. Thorvaldsdóttir, J. T. Robinson, J. P. Mesirov, Integrative Genomics Viewer (IGV): High-performance genomics data visualization and exploration. *Brief. Bioinform.* **14**, 178–192 (2013).
52. W. McLaren, L. Gil, S. E. Hunt, H. S. Riat, G. R. Ritchie, A. Thormann, P. Flicek, F. Cunningham, The ensembl variant effect predictor. *Genome Biol.* **17**, 122 (2016).
53. R. Rajaby, Y. Zhou, Y. Meng, X. Zeng, G. Li, P. Wu, W.-K. Sung, SurVirus: A repeat-aware virus integration caller. *Nucleic Acids Res.* **49**, e33–e33 (2021).
54. L.-H. Zhao, X. Liu, H.-X. Yan, W.-Y. Li, X. Zeng, Y. Yang, J. Zhao, S.-P. Liu, X.-H. Zhuang, C. Lin, Genomic and oncogenic preference of HBV integration in hepatocellular carcinoma. *Nat. Commun.* **7**, 12992 (2016).

Acknowledgments: We thank the individuals who participated in the studies. We sincerely appreciate Y. Zhang and J. Liu for help with collecting human samples. We sincerely appreciate E. Wang for help with developing the analytic pipeline. **Funding:** This study was supported by National Key R&D Program of China (2021YFC2500900 to Y.J.), National Natural Science Foundation Fund (82225033 to Y.J.), National Key R&D Program of China (2021YFC2501004 to Y.J.), State Key Projects Specialized on Infectious Diseases (2017ZX10201201-006 to C.Q. and 2017ZX10201021-007-003 to H.Z.), and the Chinese Academy of Medical Sciences (CAMS) Innovation Fund for Medical Sciences (CIFMS) (2021-1-I2M-018 to Y.J., 2021-I2M-1-067 to Y.J., 2021-I2M-1-066 to H.Z., and 2021-1-I2M-012 to H.Z.). **Author contributions:** Y.J. designed the experiments. Y.J., H.Z., and C.Q. supervised the study and provided funding. P.W. and W.Z. developed and optimized the experiment part of the MCP technology; P.W. and J.R. applied the MCP technology to the standard reference samples and clinical samples; J.R. performed experiments on other technologies (including bisulfite and hybridization capture-based sequencing) to compare the performance with the MCP technology. Q.S. developed the bioinformatic pipeline to analyze the MCP sequencing data; Q.S. and L.Z. applied the pipeline on the MCP data of all the samples and set up the HCC detection model. Q.S., L.Z., L.J., and B.Z. analyzed the performance (sensitivity, specificity, etc.) of the MCP profiling and the HCC detection model and performed the statistics analysis. H.Z., C.Q., W.C., Y.W., L.J., D.W., and K.C. collected samples and clinical information. Y.J., C.Q., P.W., Q.S., J.R., and W.Z. drafted and revised the manuscript with help from L.Z. and B.Z. All authors read and approved the final manuscript. **Competing interests:** Y.J. is one of the cofounders and has owner interest in Genetron Holdings and receives royalties from Genetron. Y.J., C.Q., P.W., and Q.S. have filed patents/patent applications (Construction and sequencing data analysis method for ctDNA library for simultaneously detecting various common mutations in liver cancer, no. WO2020007089A1 and Method for detecting mutation and methylation of tumor specific gene in ctDNA, no. WO2021073490A1) based on the technology and data generated from this work. **Data and materials availability:** The raw sequencing data were deposited in the Genome Sequence Archive for Human (GSA-Human) with the accession number HRA002276 and are available for research purpose. All data associated with this study are present in the paper or the Supplementary Materials. Computer code and scripts were archived in Zenodo with an associated DOI (10.5281/zenodo.7106903).

Submitted 7 March 2022
Resubmitted 30 May 2022
Accepted 4 October 2022
Published 23 November 2022
10.1126/scitranslmed.abp8704

Downloaded from https://www.science.org on November 25, 2022

Science Translational Medicine

Simultaneous analysis of mutations and methylations in circulating cell-free DNA for hepatocellular carcinoma detection

Pei WangQianqian SongJie RenWeilong ZhangYuting WangLin ZhouDongmei WangKun ChenLiping JiangBochao ZhangWanqing ChenChunfeng QuHong ZhaoYuchen Jiao

Sci. Transl. Med., 14 (672), eabp8704. • DOI: 10.1126/scitranslmed.abp8704

Parallel profiling for HCC detection

Cell-free DNA (cfDNA) is a useful noninvasive approach for cancer diagnostics; however, low yielding samples and smaller alteration frequencies make multiple biomarker testing difficult on single samples. Here, Wang *et al.* have developed the Mutation Capsule Plus (MCP) technology that allows for parallel profiling of mutations and methylation changes on a single cfDNA sample from patients with hepatocellular carcinoma. They validated their model on retrospective and prospective cohorts with high sensitivity and specificity. This represents a promising technology that could improve discovery and validation of biomarkers using cfDNA for many types of cancer.—DH

View the article online
https://www.science.org/doi/10.1126/scitranslmed.abp8704
Permissions
https://www.science.org/help/reprints-and-permissions

Downloaded from https://www.science.org on November 25, 2022

Use of this article is subject to the Terms of service

Science Translational Medicine (ISSN) is published by the American Association for the Advancement of Science. 1200 New York Avenue NW, Washington, DC 20005. The title *Science Translational Medicine* is a registered trademark of AAAS.
Copyright © 2022 The Authors, some rights reserved; exclusive licensee American Association for the Advancement of Science. No claim to original U.S. Government Works